Journal of Electroanalytical Chemistry 933 (2023) 117278

Contents lists available at ScienceDirect

Journal of Electroanalytical Chemistry

journal homepage: www.elsevier.com/locate/jelechem

Template-free nanostructured poly-3-hexylthiophene (P3HT) films via single pulse-nucleated electrodeposition

S.C. Perry [a,*], S. Arumugam [b], S. Beeby [b], I. Nandhakumar [a]

[a] Department of Chemistry, University of Southampton, Southampton SO17 1BJ. UK
[b] School of Electronics and Computer Science, University of Southampton, Southampton SO17 1BJ, UK

ARTICLE INFO

Keywords:
Poly-3-hexylthiophene
P3HT
Electrodeposition
Nanostructure
Conducting polymers

ABSTRACT

A template-free method for the electrochemical deposition of poly(3-hexylthiophene) (P3HT) has been demonstrated. Electrodeposition is preceded by an electrochemical nucleation step, which is essential in producing an even film over the electrode surface without needing any pre-treatment of the electrode surface through surface coatings or self-assembled monolayers. The produced film is highly nanostructured, being made up of interconnected wire-like structures on the order of 100 nm, and readily delaminates as an intact film for straightforward analysis. The films are also highly conductive without needing post-treatment or chemical dopants. This technique offers a simple route to conductive organic films for thermoelectric generators, organic solar cells or field effect transistors.

1. Introduction

Poly-3-hexylthiophene (P3HT) is a conjugated organic polymer with inherently good conductivity, making it an interesting material for a broad scope of applications including flexible thermoelectric generators [1,2], organic solar cells [3,4], organic LEDs [5] and field effect transistors [6]. Efforts to improve the P3HT's conductivity include synthetic changes and post processing, with factors such as molecular weight [7], side chain structure [8], doping [9] and annealing [10] all giving notable changes to the manufactured film's conductivity.

A number of reports have shown improved performance for nanostructured P3HT versus the equivalent amorphous film [11,12]. Several methods for P3HT nanowire formations have been investigated, such as controlled seeding [13], electrospinning [14] or crystallisation from poor solvents [15]. Recent works have also suggested that electrochemical methods for P3HT synthesis give access to a final polymer with a higher degree of electrical conductivity [16]. Electrodeposition has been demonstrated as a facile route to conductive polymer films, where precursor monomers are oxidised electrochemically alongside a coupling reaction, resulting in film growth [17]. The electrochemical method offers control of key characteristics such as film thickness and morphology through the selection of appropriate experimental parameters, including but not limited to potential waveform, total charge and components within the deposition bath.

Despite this, very few works have investigated the direct electrochemical synthesis of P3HT films from the 3-hexylthiophene monomer [18–20]. This is likely due to the challenge of creating even films over the surface of the electrode, since most published examples of 3-hexylthiophene electropolymerisation require a careful pre-treatment of the electrode surface in order to facilitate the initial deposition. This has been done with self-assembled monolayers of a thiol-precursor [20,21] or through transfer of an epitaxially grown thin polymer layer onto the electrode so that the polymer is already smooth and complete before the electrodeposition begins [17,22]. Of these, the electrochemical synthesis of nanostructured P3HT invariably requires the use of a template, most commonly porous alumina, in order to guide the formation of nanowires or nanorods [23,24]. This technique is effective, but comes with well documented challenges associated with pore filling and template removal after the deposition [25].

Here, we demonstrate a new route to the template-free electrochemical deposition of nanostructured P3HT films. Deposition is facilitated with an initial anodic pulse to give a broad coating of nucleation sites that results in an even deposition across the entire electrode surface without the need for a self-assembled monolayer or similar pre-treatment designed to facilitate deposition at the ITO surface. Subsequent electrodeposition via cyclic voltammetry produces a film that is highly nanostructured and highly conductive without any additional post-treatment or chemical doping. Additionally, we demonstrate that the P3HT can be simply transferred onto a non-conductive flexible

* Corresponding author.
E-mail address: iris@soton.ac.uk (I. Nandhakumar).

https://doi.org/10.1016/j.jelechem.2023.117278
Received 11 December 2022; Received in revised form 16 February 2023; Accepted 17 February 2023
Available online 20 February 2023

substrate, giving our technique applications for the fabrication of flexible power generation devices through thermoelectric or photovoltaic applications.

2. Material and methods

Electrodeposition solutions of 100 mM 3-hexylthiophene (Sigma-Aldrich, 98%) and 100 mM tetrabutylammonium hexafluorophosphate ($TBAPF_6$) (Sigma-Aldrich, 99%) in acetonitrile (Sigma-Aldrich, 99.8%) were made in a in a nitrogen-filled flow box (Cleaver Scientific). Indium tin oxide (ITO) working electrodes were prepared by cutting ITO coated class slides (Ossila) into 1.5 × 1 cm pieces and connecting to a copper wire using silver epoxy (RS Components) and curing at 80 °C overnight. Electrodes were cleaned by sonicating in Decon® detergent, water and isopropyl alcohol sequentially for 15 mins before drying under nitrogen.

Solutions were transferred into a sealed glass vial along with ITO working electrode, platinum wire counter electrode, and Ag/Ag^+ reference electrode, which were fabricated in house. The reference electrode was fabricated by immersing a 1 mm diameter silver wire in 10 mM $AgNO_3$ (Sigma-Aldrich, 99%) and 100 mM $TBAPF_6$ in acetonitrile within a fritted glass body. The reference was calibrated using a standard procedure [26], by measuring the standard redox potential for the ferrocene/ferrocenium couple (2.5 mM) in 100 mM $TBAPF_6$ in acetonitrile.

Electrochemical measurements and depositions were carried out using a Metrohm μAutolab Type II potentiostat, controlled using Nova 2.1. Depositions were done by cycling the ITO electrode between −0.3 V and 1.8 V vs Ag/Ag^+ at 200 mV/s. After deposition, the P3HT films were rinsed in acetonitrile and then dried under nitrogen gas.

Images of the resultant P3HT films were recorded on a Jeol JSM-7200F scanning electron microscope (SEM). Film thicknesses were determined through SEM images by taking a mean of ten measurements along the film cross section. In order to characterise the conductivity of the films without interference from the ITO electrode underneath, the P3HT films were first delaminated by firmly pressing adhesive Kapton tape (RS Components) onto the surface of the film, and then slowly peeling back to delaminate the P3HT from the ITO. Electrical conductivity was then recorded using an Ecopia HMS-3000 measurement system equipped with a four-point probe.

3. Results and discussion

The electrochemical properties of 3-hexylthiophene were first determined using cyclic voltammetry (CV) by cycling an ITO electrode in 100 mM 3-hexylthiophene solution (Fig. 1A). The first CV shows an anodic current at very positive potentials corresponding to the oxidation of the 3-hexylthiophene to P3HT. The second CV then shows two additional peaks, corresponding to the redox process of the deposited P3HT film, as well as the increased current at more positive potentials corresponding to further film growth. Continued deposition is evidenced by the continued increase in peak size over subsequent cycles.

Cyclic voltammetry under these conditions shows a significant increase in peak separation over continued cycling. Since the electrodeposited P3HT has a fairly high conductivity, this feature is likely due to resistance associated with the poor adhesion between the electrodeposited P3HT and the ITO, which is exacerbated by the moderate scan rate. Slowing the scan rate for a previously electrodeposited P3HT film on ITO reveals a characteristic shape for P3HT voltammetry with a smaller separation between the anodic and cathodic peaks (Fig. 1B). The single anodic and cathodic peak is indicative of a P3HT film with lesser ordering and/or low regioregularity [20,27].

It is worth mentioning that the poor adhesion between the electrodeposited P3HT and ITO resulted in a steady delamination of the

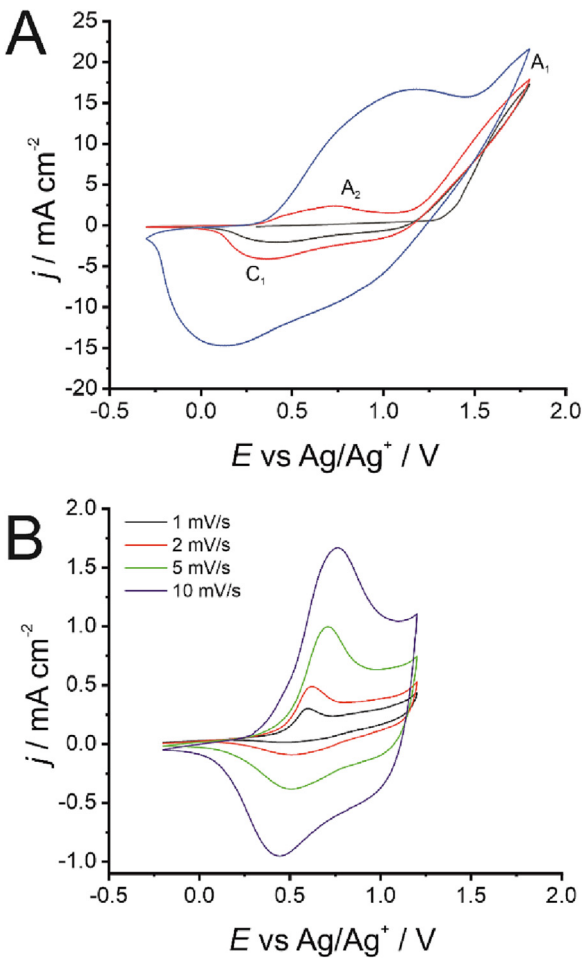

Fig. 1. A. CVs for 3-hexylthiophene electrodeposition at an ITO electrode, showing the first (black) second (red) and tenth (blue) CVs. Initial deposition occurs at very anodic potentials (A_1). Once a P3HT film is present, additional peaks are seen due to the oxidation (A_2) and reduction (C_1) of the P3HT. The growing peaks are due to the increased amount of electrochemically active P3HT at the ITO surface. CVs were recorded in 100 mM 3-hexylthiophene and 100 mM $TBAPF_6$ in acetonitrile at 200 mV/s. B. CVs for a previously electrodeposited P3HT film at 1 (black), 2 (red), 5 (green) and 10 mV/s (blue) recorded in 100 mM $TBAPF_6$ in acetonitrile.

film during repeated cycling. Relatively poor adhesion for P3HT and related polymers has previously been observed for films on ITO due to low bonding strength between the two components [28,29], with a number of works trying to address this with surface modifications or adhesion promotors that were not present in this work [30,31]. This is likely exacerbated in this works due to the electrodeposited films being thicker than those typically produced via spin coating, drop casting or dip coating. The film remained intact, but slowly peeled away from the bottom of the ITO so the front and back face were both exposed to electrolyte, while the top of the film remained intact. Care was taken to limit experimental time frames so that data were only recorded while the film remained adhered.

When growing P3HT by CV on ITO, the resultant films showed a highly uneven growth, resulting in delocalised P3HT “islands” dispersed across the electrode surface. This is because, unlike previously reported literature examples for P3HT deposition, we are not employing a surface pre-treatment or self-assembled monolayer to guide the electrodeposition of a smoother film [17,20–22]. In order to facilitate more even growth across the ITO, we instead employed a short anodic pulse to the ITO, resulting in the nucleation of electrodeposited P3HT

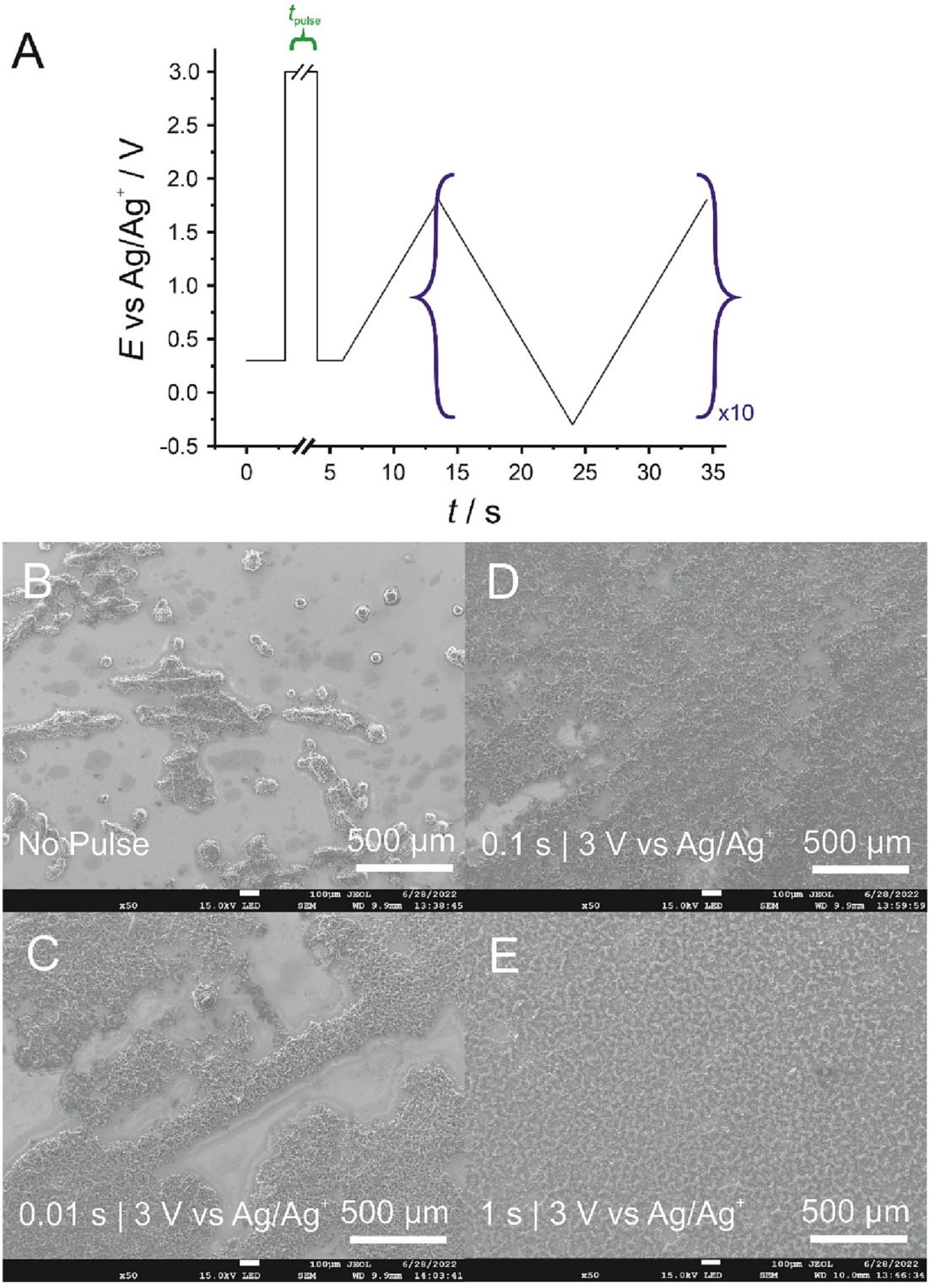

Fig. 2. A) Potential waveform used for the deposition of P3HT films at an ITO electrode. B-E) SEM images of P3HT films obtained using the waveform in A. The electrode was pulsed at 3 V vs Ag/Ag^+ for 0 s (B), 0.01 s (C), 0.1 s (D) and 1 s (E) prior to depositing P3HT by cycling 10 times between −0.3 V and 1.8 V vs Ag/Ag^+ in 100 mM 3-hexylthiophene and 100 mM $TBAPF_6$ in acetonitrile at 200 mV/s.

across its surface (Fig. 2). Cycling the nucleated ITO then resulted in much more even growth over the surface.

It is worth mentioning that other thiophene polymers have been electrodeposited without needing a pre-deposited monolayer, surface treatment or anodic pulse. One such example demonstrated that poly-3-methylthiophene (P3MT) may be electrochemically deposited by simple galvanostatic methods [32,33]. This suggests that exchanging the bulky hexyl substituent for a short methyl unit facilitates more even deposition at the ITO. It is not clear if this is due to faster mass transport of the smaller P3MT monomer or due to steric factors as the film is growing, which merits future investigation.

The timescale of the nucleation pulse (t_{pulse}) had a sizeable impact the total coverage of P3HT over the surface of the ITO. The pulse needed to be sufficiently long to drive P3HT nucleation across the ITO, without being so large as to deposit a thick coating of material rather than thin nucleation sites. Fig. 2 shows how the resultant P3HT deposition is patchy and highly dispersed in the absence of a nucleation pulse. The bare areas become progressively smaller as t_{pulse} is increased until a 1 s pulse results in more even deposition over the ITO.

The potential for the nucleation pulse (E_{pulse}) was also investigated. It is not desirable to have a highly anodic potential for long periods as this may over-oxidise the polymer. However, a highly anodic potential is necessary in order to drive the formation the nucleation layer across the ITO surface. E_{pulse} = 3 V vs. Ag/Ag^+ was therefore chosen as the least positive potential that gave a visibly smooth P3HT film after a 1 s nucleation pulse, so that the nucleation was complete without too thick a layer being deposited before the film was grown by CV. The highly anodic pulse is only necessary for the initial nucleation, not for subsequent P3HT growth once the nucleation is complete. Therefore, it was possible to grow the P3HT film via CV with a more moderate 1.8 V vs Ag/Ag^+ as the anodic limit.

The need for the nucleation pulse is due to the heterogeneous nature of ITO surfaces, with the surface being defined by the nature of the oxide, extent of hydrolysis of the lattice and the orientation of the oxide grains [34]. Electrochemical reactions will preferentially occur at active defect sites, such as oxygen vacancies, interstitial indium and substitutional tin [35]. The net result is a surface with an intrinsic variation in surface conductivity that gives locally different electrochemical reaction rates [36,37], with scanning electrochemical cell microscopy studies have found up to three orders of magnitude difference in the standard rate constant (k^0) for a model single electron transfer system [38].

The role of the anodic pulse is therefore to overcome the conductivity barrier at less conductive regions of the heterogeneous ITO surface. Without the pulse, P3HT preferentially deposits at the more conductive sites, leading to patchy growth. With the anodic pulse, sufficient overpotential is supplied to the more and less conductive site to deposit a nucleation layer of P3HT, which facilitates the growth of a smoother film over the following CVs (Fig. 3).

In order to characterise the P3HT in terms of its conductivity, the film was transferred onto non-conductive Kapton tape through a simple process of the pressing tape onto the P3HT layer and then slowly peeling it away. The relatively poor adhesion between the ITO surface and the P3HT film is advantageous in this case, since the P3HT is easily delaminated from the ITO, giving a complete film on the Kapton tape. The conductivity was found to be high at 78.9 S cm^{-1}, despite there being no additional dopant incorporated into film during post treatment. Based on a comprehensive literature search, we believe this is the highest reported conductivity for electrochemically fabricated P3HT, and compares favourably with P3HT produced by other methods such as spin coating or drop-casting (Table 1).

Although no chemical dopant was added to this P3HT film, the electrolyte present during electrodeposition has a role in facilitating P3HT conductivity. Biasing the P3HT at a positive potential, known as electrochemical doping, causes anions to migrate into the P3HT and therefore drives a charge build-up within the film [48,49]. The electrolyte is therefore chosen so that the anion may penetrate and remain within the film in order to give an efficient stabilisation of the doped P3HT states [50]. For this reason, the deposition waveform is always ended at the positive potential limit.

Despite the film produced here being significantly thicker than most published examples of P3HT (4.97 μm), the high conductivity indicates effective incorporation of PF_6^- anions throughout the film structure. Closer analysis of the electrodeposited P3HT revealed a highly nanostructured morphology (Fig. 4). The structure appears to be made up of a network of wire-like structures, with diameters on the order of 100 nm, that are all highly interconnected.

Similarly magnified images of the films produced in the absence of the pulse revealed much denser deposits, with the film becoming increasingly fibrous as the pulse length increases. Although the pulse length clearly does impact the nanostructure of the resultant film, it is unclear of the precise mode of this impact. It may be that the nucle-

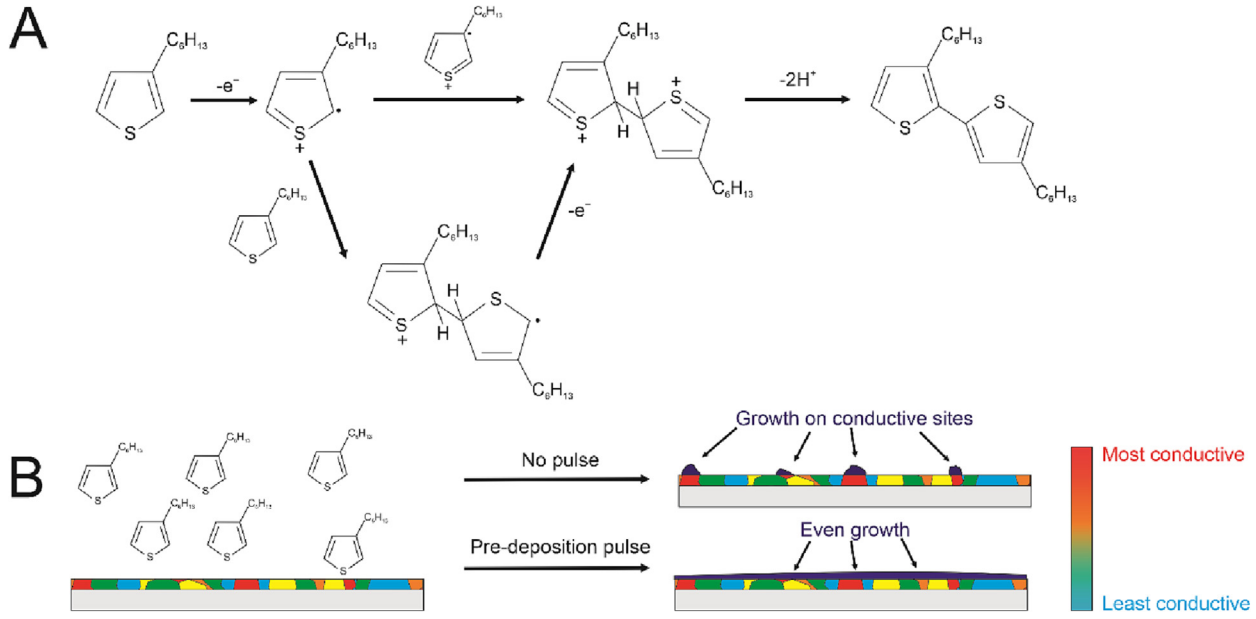

Fig. 3. A) Mechanism for P3HT electrodeposition. The 3-hexylthiophene is initial oxidised by a single electron transfer. Polymerisation can then occur either via a radical coupling (top path) or by reaction between radical and monomer, followed by a further single electron oxidation of the resultant cation (bottom path) [39]. B) Schematic representation of P3HT oxidation at a heterogeneous ITO surface. Colours of the ITO represent the conductivity, where red sites are most conductive and blue are least conductive. Without the anodic pulse, electrodeposition occurs preferentially at the more conductive (red) sites. With the anodic pulse, an initial nucleation layer is deposited across the ITO, so subsequent growth by CV can give more complete coverage.

Table 1
Conductivity of P3HT from this work compared to other published examples from literature. Quoted values are all for disordered P3HT, and do not include highly oriented P3HT, where alignment through small-molecule epitaxy [40] or high-temperature rubbing [41] gives higher conductivity in one single direction. Quoted dopants include fluorinated tetracyanoquinodimethane (F_4TCNQ), iron tris(trifluoromethylsulfonyl)imide ($Fe(TFSI)_3$), molybdenum tris(1,2-bis(trifluoromethyl)ethane-1,2-dithiolene) ($Mo(TFD)_3$) and (tridecafluoro-1,1,2,2,-tetrahydrooctyl)-trichlorosilane (FTS).

Method	Dopant	σ/S cm^{-1}	Reference
Alumina templated electrodeposition	F_4TCNQ	6.25	[11]
Spin coating	F_4TCNQ	12.7	[42]
Drop casting	FTS	27.7	[43]
Spin coating	$FeCl_3$	42	[44]
Spin coating	F_4TCNQ	48	[9]
Spin coating	Mo $(TFD)_3$ + $FeCl_3$	68.5	[45]
Pulse-nucleated electrodeposition	PF_6^-	78.9	This work
Drop casting	$Fe(TFSI)_3$	87	[46]
Drop casting	$FeCl_3$	128	[47]

ation sites produced by the longer pulse are more suited to the production of this fibrous structure.

Alternatively, it may be due to the impact of deposition occurring more sporadically at surfaces that have not been nucleated by the pre-deposition pulse. The solution environment for deposition at a sparely deposited ITO surface could be expected to be different compared to one where deposition is more even across the ITO surface, with the isolated islands of P3HT deposition giving a distinct nanostructure compared to where P3HT is electrodeposited more evenly. Since other literature examples of electrochemically deposited polythiophenes have not revealed similar structures, it seems likely that the former is the case, though we cannot discount some impact from the latter.

Although thick films were chosen here for ease of analysis, the inherent flexibility of electrochemical techniques allows this same concept to be applied to thinner films through changes in the deposition conditions. Large magnitude changes are possible through variation in 3-hexylthiophene concentration, CV scan speed or potential deposition range, then the film thickness is simply controlled by changing the number of cycles.

It is worth noting that the cross section of the film seen in Fig. 4I shows that the distribution of these P3HT fibres is not perfectly homogeneous. Some of this may be due to damage during the production and imaging of the cross section, although other elements may be due to the deposition procedure itself. The overall coverage of the P3HT is dependent on the pulse conditions, and the overall film quality will also depend on a broad scope of parameters, including the CV range, scan rate, 3-hexylthiophene concentration, and the conductivity of the ITO itself. It is likely this cross section could be made more homogenous through a complete parameterisation of these parameters, and this work is ongoing as part of efforts to use this technique in device fabrication.

Other useful conductive organic polymers are also accessible through electrochemical deposition, such as polypyrrole (PPy) [51], polyaniline (PANi) [52] or poly(3,4-ethylenedioxythiophene) (PEDOT) [53]. This template-free route to nanostructured conductive polymers is therefore applicable to a broad scope of interesting conductive polymers, requiring only a change in deposition monomer and optimisation of the pre-deposition pulse waveform.

4. Conclusions

We have demonstrated the template-free production of a highly nanostructured film of P3HT using electrochemical deposition. Unlike previous examples where the electrode surface is pre-treated with a surface modification specifically designed to facilitate electrodeposition, we demonstrate that a highly anodic pulse is sufficient to

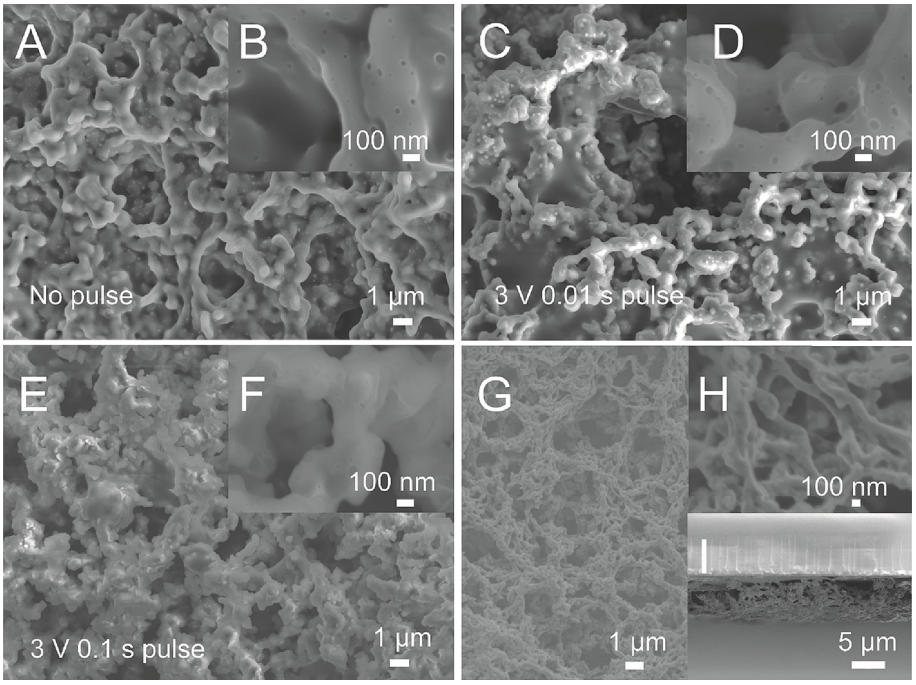

Fig. 4. SEM images of the surface of the electrodeposited P3HT film at 5,000x and 45,000x magnification for films with no pulse (A and B), 0.01 s pulse (C and D), 0.1 s pulse (E and F) and 1 s pulse (G and H) respectively. Images were taken of the as-deposited film on the ITO surface prior to delamination. Image of the cross section (I) of the 1 s pulse film was taken by scoring the back of the ITO-coated glass with a diamond scribe, and then breaking the glass and film together. Deposition was done in 100 mM 3-hexylthiophene and 100 mM $TBAPF_6$ in acetonitrile by pulsing the potential at 3 V vs. Ag/Ag^+ for 1 s, then cycling 10 times between −0.3 V and 1.8 V vs Ag/Ag^+ at 200 mV/s. Images correspond to the surface of the P3HT film prior to delamination.

nucleate the surface of the electrode, which then permits a more complete subsequent P3HT electrodeposition over the electrode surface.

As well as being highly nanostructured, the deposited film shows a good conductivity without any post-treatment or doping. This appears to be due to the *in situ* incorporation of PF_6^- counterions from the electrolyte during the deposition, which acts to stabilise charge carriers within the P3HT structure. This technique is applicable to a broad scope of alternative conductive polymers through selection of an appropriate electrochemically active monomer, representing a quick and simple route to nanostructured conductive polymers for a broad range of applications.

CRediT authorship contribution statement

S.C. Perry: Writing – review & editing. **S. Arumugam:** Investigation. **S. Beeby:** Funding acquisition. **I. Nandhakumar:** Funding acquisition, Project administration, Supervision, Writing – review & editing.

Declaration of Competing Interest

The authors declare that they have no known competing financial interests or personal relationships that could have appeared to influence the work reported in this paper.

Acknowledgements

This work was financially supported by the Engineering and Physical Sciences Research Council (EPSRC) Grant No. EP/T026219/1. The authors would also like to thank the University of Southampton Glassblowers for producing custom fritted glass electrode bodies for reference electrode fabrication.

References

[1] B. Russ, A. Glaudell, J.J. Urban, M.L. Chabinyc, R.A. Segalman, Nat. Rev. Mater. 1 (2016) 16050.
[2] M. Culebras, K. Choi, C. Cho, Micromachines 9 (2018) 638.
[3] E. L. Lim, C. C. Yap, M. A. Mat Teridi, C. H. Teh, A. R. b. Mohd Yusoff and M. H. Hj Jumali, *Org. Electron.*, 2016, **36**, 12-28.
[4] C. Liu, K. Wang, X. Gong, A.J. Heeger, Chem. Soc. Rev. 45 (2016) 4825–4846.
[5] J. Liang, L. Li, X. Niu, Z. Yu, Q. Pei, Nat. Photon. 7 (2013) 817–824.
[6] J. Yang, Z. Zhao, S. Wang, Y. Guo, Y. Liu, Chem 4 (2018) 2748–2785.
[7] S. Qu, Q. Yao, B. Yu, K. Zeng, W. Shi, Y. Chen, L. Chen, Chem. Asian J. 13 (2018) 3246–3253.
[8] P.A. Finn, I.E. Jacobs, J. Armitage, R. Wu, B.D. Paulsen, M. Freeley, M. Palma, J. Rivnay, H. Sirringhaus, C.B. Nielsen, J. Mater. Chem. C 8 (2020) 16216–16223.
[9] E. Lim, K.A. Peterson, G.M. Su, M.L. Chabinyc, Chem. Mater. 30 (2018) 998–1010.
[10] K. Gu, Y. Wang, R. Li, E. Tsai, J.W. Onorato, C.K. Luscombe, R.D. Priestley, Y.-L. Loo, ACS Appl. Mater. Interfaces 13 (2021) 999–1007.
[11] J. Hu, K.W. Clark, R. Hayakawa, A.-P. Li, Y. Wakayama, Langmuir 29 (2013) 7266–7270.
[12] S. van Bavel, E. Sourty, G. de With, K. Frolic, J. Loos, Macromolecules 42 (2009) 7396–7403.
[13] W. Hourani, K. Rahimi, I. Botiz, F.P. Vinzenz Koch, G. Reiter, P. Lienerth, T. Heiser, J.-L. Bubendorff, L. Simon, Nanoscale 6 (2014) 4774–4780.
[14] J.-Y. Chen, H.-C. Wu, Y.-C. Chiu, C.-J. Lin, S.-H. Tung, W.-C. Chen, Adv. Electron. Mater. 1 (2015) 1400028.
[15] K. Tang, L. Huang, J. Lim, T. Zaveri, J.D. Azoulay, S. Guo, A.C.S. Appl, Polym. Mater. 1 (2019) 2943–2950.
[16] D. Pourjafari, A. Vazquez, J. Cavazos, I. Gomez, Soft Mater. 12 (2014) 380–386.
[17] Z. Ren, X. Zhang, H. Li, X. Sun, S. Yan, Chem. Commun. 52 (2016) 10972–10975.
[18] S. Gáspár, T. Ravasenga, R.-E. Munteanu, S. David, F. Benfenati, E. Colombo, Materials 14 (2021) 4761.
[19] B. Endrődi, G.F. Samu, M.A. Azam, C. Janáky, C. Visy, J. Solid State Electrochem. 20 (2016) 3179–3187.
[20] E.L. Ratcliff, J.L. Jenkins, K. Nebesny, N.R. Armstrong, Chem. Mater. 20 (2008) 5796–5806.
[21] Y. Lv, L. Yao, C. Gu, Y. Xu, D. Liu, D. Lu, Y. Ma, Adv. Func. Mater. 21 (2011) 2896–2900.
[22] D. Sun, Y. Li, Z. Ren, M.R. Bryce, H. Li, S. Yan, Chem. Sci. 5 (2014) 3240–3245.
[23] D. Pourjafari, T. Serrano, B. Kharissov, Y. Peña, I. Gómez, Int. J. Mater. Res. 106 (2015) 414–420.
[24] R. Xiao, S.I. Cho, R. Liu, S.B. Lee, J. Am. Chem. Soc. 129 (2007) 4483–4489.
[25] J. Heinze, B.A. Frontana-Uribe, S. Ludwigs, Chem. Rev. 110 (2010) 4724–4771.
[26] V.V. Pavlishchuk, A.W. Addison, Inorg. Chim. Acta 298 (2000) 97–102.
[27] M. Skompska, A. Szkurłat, Electrochim. Acta 46 (2001) 4007–4015.
[28] Y. Wei, J.-M. Yeh, D. Jin, X. Jia, J. Wang, G.-W. Jang, C. Chen, R.W. Gumbs, Chem. Mater. 7 (1995) 969–974.
[29] C.-Y. Lai, P.J.S. Foot, J.W. Brown, Polym. Polym. Compos. 25 (2017) 119–128.
[30] S. Kim, L.K. Jang, H.S. Park, J.Y. Lee, Sci. Rep. 6 (2016) 30475.
[31] A.M. Kumar, M.A. Hussein, A.Y. Adesina, S. Ramakrishna, N. Al-Aqeeli, RSC Adv. 8 (2018) 19181–19195.
[32] R. Valaski, L.S. Roman, L. Micaroni, I.A. Hümmelgen, Eur. Phys. J. E 12 (2003) 507–511.
[33] J. Roncali, A. Yassar, F. Garnier, J. Chem. Soc. Chem. Commun. (1988) 581–582.
[34] S. Shen, X. Zhang, S. Mubeen, M.P. Soriaga, J.L. Stickney, Electrochim. Acta 316 (2019) 105–112.
[35] T.S. Bejitual, K. Ramji, A.J. Kessman, K.A. Sierros, D.R. Cairns, Mater. Chem. Phys. 132 (2012) 395–401.
[36] P. Ciocci, J.-F. Lemineur, J.-M. Noël, C. Combellas, F. Kanoufi, Electrochim. Acta 386 (2021) 138498.
[37] N.Y. Molina, T. Pungsrisai, Z.J. O'Dell, B. Paranzino, K.A. Willets, ChemElectroChem 9 (2022) e202200245.
[38] O.J. Wahab, M. Kang, G.N. Meloni, E. Daviddi, P.R. Unwin, Anal. Chem. 94 (2022) 4729–4736.
[39] R.M.G. Rajapakse, D.L. Watkins, T.A. Ranathunge, A.U. Malikaramage, H.M.N.P. Gunarathna, L. Sandakelum, S. Wylie, P.G.P.R. Abewardana, M.G.S.A.M.E.W.D.D. K. Egodawele, W.H.M.R.N.K. Herath, S.V. Bandara, D.R. Strongin, N.H. Attanayake, D. Velauthapillai, B.R. Horrocks, RSC Adv. 12 (2022) 12089–12115.
[40] S. Qu, Q. Yao, L. Wang, Z. Chen, K. Xu, H. Zeng, W. Shi, T. Zhang, C. Uher, L. Chen, npj Asia Mater. 8 (2016) e292–e.
[41] V. Vijayakumar, Y. Zhong, V. Untilova, M. Bahri, L. Herrmann, L. Biniek, N. Leclerc, M. Brinkmann, Adv. Energy Mater. 9 (2019) 1900266.
[42] J. Hynynen, D. Kiefer, L. Yu, R. Kroon, R. Munir, A. Amassian, M. Kemerink, C. Müller, Macromolecules 50 (2017) 8140–8148.
[43] A.M. Glaudell, J.E. Cochran, S.N. Patel, M.L. Chabinyc, Adv. Energy Mater. 5 (2015) 1401072.
[44] I.H. Jung, C.T. Hong, U.-H. Lee, Y.H. Kang, K.-S. Jang, S.Y. Cho, Sci. Rep. 7 (2017) 44704.
[45] Z. Liang, Y. Zhang, M. Souri, X. Luo, A.M. Boehm, R. Li, Y. Zhang, T. Wang, D.-Y. Kim, J. Mei, S.R. Marder, K.R. Graham, J. Mater. Chem. A 6 (2018) 16495–16505.
[46] Q. Zhang, Y. Sun, W. Xu, D. Zhu, Energy Environ. Sci. 5 (2012) 9639–9644.
[47] L. Wu, H. Li, H. Chai, Q. Xu, Y. Chen, L. Chen, ACS Appl. Electron. Mater. 3 (2021) 1252–1259.
[48] D. Rawlings, E.M. Thomas, R.A. Segalman, M.L. Chabinyc, Chem. Mater. 31 (2019) 8820–8829.
[49] M. Rudolph, E.L. Ratcliff, Nat. Commun. 8 (2017) 1048.
[50] D. Neusser, C. Malacrida, M. Kern, Y.M. Gross, J. van Slageren, S. Ludwigs, Chem. Mater. 32 (2020) 6003–6013.
[51] J. El Nady, A. Shokry, M. Khalil, S. Ebrahim, A.M. Elshaer, M. Anas, Sci. Rep. 12 (2022) 3611.
[52] D.M. Wirth, L.J. Waldman, M. Petty, G. LeBlanc, J. Electrochem. Soc. 166 (2019) D635.
[53] J.A. Del-Oso, B.A. Frontana-Uribe, J.-L. Maldonado, M. Rivera, M. Tapia-Tapia, G. Roa-Morales, J. Solid State Electrochem. 22 (2018) 2025–2037.